Demonstration of Simultaneous Quad-Polarization SAR Imaging for Extended Targets in MIMO-SAR

Tobias Rommel, Marwan Younis and Gerhard Krieger
German Aerospace Centre (DLR)
82234 Wessling
Email: tobias.rommel@dlr.de

***Abstract*—Due to a high demand for global Synthetic Aperture Radar (SAR) data sets, recent spaceborne sensors reach their limits in terms of resolution, swath width and repeat cycle. In addition, fully polarimetric operation reduces the maximum swath width approximately by the factor of two. To solve SAR inherent limitations, a new generation of sensors with multiple transmit and multiple receive channels (MIMO) and digital beam-forming (DBF) capabilities is suggested. Using a quad-polarized MIMO-SAR, transmitting simultaneously orthogonal waveforms in horizontal and vertical polarizations, enables data acquisitions without any reduction of the swath width or resolution. In this paper a concept is described, which uses an advanced filtering and processing method to separate the transmitted signals in the receiver and to measure all four parameters of the scattering matrix simultaneously. Ground-based MIMO-SAR measurement results are presented, which serve as a first verification of the suggested technique with an extended, non point-like target.**

I. INTRODUCTION

Since the first developments of Synthetic Aperture Radar (SAR) by Carl Wiley in 1951, radar for imaging applications has become an important remote sensing technique over the past decades. Manifold applications reaching from climate change research, over change detection and 4-D mapping up to security-related applications are served. Especially high-resolution, day-and-night and weather-independent imaging capabilities led to the success of recent spaceborne SAR missions, like COSMO-SkyMed, TerraSAR-X/TanDEM-X, Radarsat-2 or Sentinel-1 [1], [2], [3]. However, the steady demand for recordings with higher resolutions, wider coverage, increased flexibility and shorter repetition intervals, brings the state-of-the-art SAR sensors to their limitations. These limitations are mainly caused by the well known contradicting requirement, of SAR system design, where the swath width limits the resolution in azimuth and vice versa [4]. If they are not considered, ambiguities will arise.

SAR sensors with Digital Beam-Forming (DBF) capabilities have promising properties to overcome this limitation. The overall idea is to suppress range ambiguities by steering the receive antenna beam to different directions in elevation [5]. With a posteriori spatiotemporal filtering it becomes possible to separate the near and far echoes arriving at the SAR platform at the same time. The swath-width can then be chosen nearly independently of the Pulse Repetition Frequency (PRF), enabling a high azimuth resolution. In addition, multiple transmit channels can be used to enhance the capabilities of the sensor [6], [7]. With such a Multiple-Input Multiple-Output (MIMO) SAR, arbitrary waveforms can be transmitted in arbitrary directions and polarization states at the same time. Finally, promising advantages of MIMO-SAR will result in a more flexible system operation and application of new advanced imaging methods, such as simultaneous quad-polarization.

Up to now, these methods have been just verified by measurements with dedicated point targets [8]. Due to cross-correlation interferences from the other transmit waveforms caused by established de-correlation methods, there is hardly any impact on the observed scene. However, extended homogenous targets consist of a large number of point scatterers and the interfering energy will sum up for every single point on the swath. In the end, these unwanted energy contributions are too strong and will be visible in the SAR image. To show that the advanced processing and de-correlation technique presented in this paper is able to handle this issue, an experiment with a fence as extended target was conducted.

The paper is structured as follows: At the beginning, a brief explanation of the state-of-the-art quad-polarization technique in SAR is given. The same section presents also the suggested MIMO idea for simultaneous quad-polarization. Afterwards, a concept using orthogonal waveforms and spatiotemporal filtering is described, which enables to separate the overlaid echo signals from different transmitters. This is followed by information about the MIMO-SAR demonstrator and measurement setup used for verification of the suggested technique for extended targets. The paper ends with measurement results and the conclusion.

II. QUAD-POLARIZATION

One advantage of MIMO-SAR is to perform fully polarimetric SAR measurements. With the use of polarimetry, the classification of man-made and natural scatterers by obtaining orientation, dielectric properties and shape of the scatterer, becomes possible. Striking examples for that are the estimation of soil moisture and the classification of biomass [9]. However, to obtain all four parameters of the scattering matrix (for example: HH, HV, VH, VV), four independent measurements have to be taken. At the current state, the sensor transmits in horizontal (H) and vertical (V) polarization in an interleaved mode. Two orthogonal polarizations are received and recorded simultaneously. Thus, to keep the azimuth sampling rate the same, the PRF has to be increased by a factor of two, which decreases the swath-width approximately by the same factor. Consequently, the simultaneous acquisition of the whole scattering matrix at full swath width would be a tremendous advantage. With the MIMO method firstly proposed in [10], both polarizations can be transmitted at the same time with non-interfering waveforms, whereas the whole scattering matrix will be obtained later in the receiver with an innovative beam-forming algorithm. As a result, the swath-width can be kept constant for quad-polarization. The necessary algorithm is described in the next section.

III. Orthogonal Waveforms and Space-Time-Frequency Adaptive Processing

For MIMO-SAR signals, or in general, for imaging radar signals, orthogonality is not only required for a certain point of time, but also for arbitrary shifts between the signals. The reason lies in cross-correlation interferences, which cannot be accepted in SAR. When observing extended areas, the energy of all transmitted signals is spread over time. Thus, conventional waveforms and post processing techniques will fail. The only way to remove the unwanted energy from the other waveforms is by using transmit signals with certain correlation characteristics in combination with a spatial filter.

One example for a suitable waveform is the multiple sub-pulse mode [11]. Basically, it is a pulse train of equal chirp signals, while each sub-pulse shares the full signal bandwidth. This is graphically depicted in Fig. 1 for two transmit channels. It should be noted, that the pulses are not transmitted at the same time and it is thus not a true MIMO mode. To still justify the expression MIMO in that case, the echoes of adjacent transmitted pulses will overlap because of the large time-dispersivity within the channels and the receiver can not distinguish between the equal-shaped transmit signals with standard processing methods.

Hence, it is necessary to form multiple receive antenna beams at the same time, which follow each transmitted sub-pulse individually. Because both sub-pulses have the same shape and a unique separation can still not be provided with DBF, additional bandpass-filters are used. This enables to form frequency dispersive antenna beams (Fig. 2). Afterwards the pre-filtered receive signals are combined in a way that two raw data streams are generated, where each contains the echo of one of the transmitted sub-pulses. Since the definite relation between Angle of Arrival (AoA), Time of Arrival (ToA) and frequency is exploited, this filtering technique is named Space-Time-Frequency Adaptive Processing (STFAP).

IV. MIMO-SAR Demonstrator

To verify the suggested quad-polarization mode and other DBF and MIMO concepts, a ground-based MIMO-SAR has been developed (Fig. 3). First polarimetric measurement results have already been presented in [8]. The radar is operating in X-band at a center frequency of 9.58 GHz and with a maximum signal bandwidth of B = 300 MHz. In its basic configuration, the radar operates with four independent

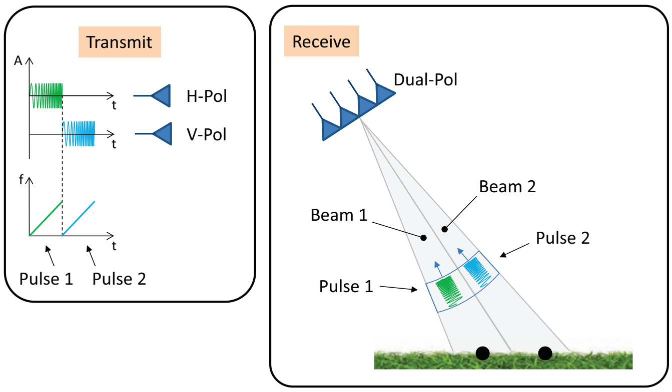

Fig. 1. Spatiotemporal filtering of sub-pulses. The echoes of the time shifted transmit waveforms overlap in the channel and are received simultaneously.

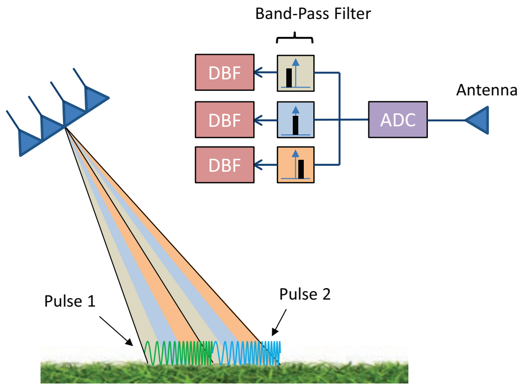

Fig. 2. Principle of frequency dispersive antenna beams on receive.

transmit and eight independent receive channels. The modular design in 19" form and full-coherent system design via a single shared 1.0 GHz LO (Local Oscillator) clock signal allows great flexibility for system changes and extensions to more transmit and receive channels or other frequency bands. The radar system itself is mounted on a motorized platform, which is moving with a constant velocity of 0.10 m/s (max. 0.98 m/s possible) along rails. To imitate the side-looking geometry of a spaceborne SAR, an antenna carrier of 6.5 m height is used.

The four dual-polarized patch antennas are connected to all eight receive channels and have an element spacing of 1.6 λ along elevation, while λ is the carrier wavelength of 3.1 cm. After combination with DBF, the Half-Power Beam-Width (HPBW) of the synthesized beam will be 10.1°, while the minimum angular separation of the grating lobes is 49°. This ensures that grating lobes are outside the observed area of interest and that sequentially transmitted sub-pulses can be traced with individual receive beams.

V. Measurement Scenario and Processing

The measurement was conducted on a meadow with the previously described MIMO-SAR demonstrator. As distributed

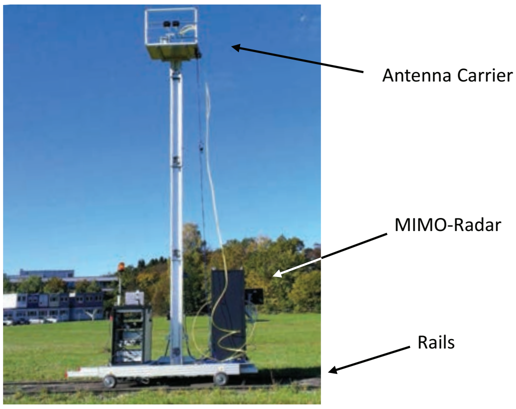

Fig. 3. MIMO-SAR demonstrator.

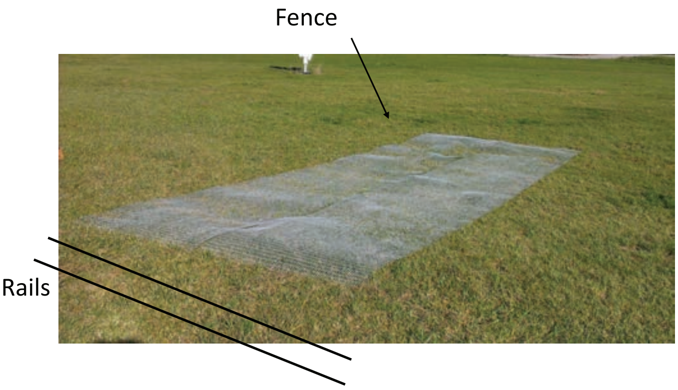

Fig. 4. Measurement scene containing a fence of size 4.0 m x 10.0 m.

target served a fence of size 4.0 m x 10.0 m and a grid size of 2.5 cm x 5.0 cm. A picture is given in Fig. 4.

Since two transmit channels are sufficient (one channel for H-polarization and one for V-polarization), only two sub-pulses are transmitted per pulse repetition interval. To test the potential of STFAP, very short pulses of duration $\tau_{\mathrm{p}} = 0.3\ \mu$s were used. This leads not only to an overlap of the echos for the observed area, but also to a low transmitted amount of energy. To circumvent this loss of energy and to get a higher SNR, the PRF was increased.

According to the suggested STFAP concept, two receive antenna beams are formed by DBF, while each sub-pulse is traced by its own beam. However, the seen pulse length of $> \tau_{\mathrm{p}} \cdot \mathrm{c}_0/2 = 45.0$ m is greater than the antenna HPBW of 10.1° after DBF combination and a pulse extension loss might result [12]. With the used STFAP technique broad frequency dispersive antenna beams are formed and the loss will not occur. Each receive channel was divided into three sub-channels, while each sub-channel shared one third of the full signal bandwidth (Fig. 2). This is done for the horizontal and vertical receive channels individually to get four independent data sets, which correspond to the HH, HV, VH and VV polarization states of the scattering matrix. This is followed by standard SAR processing steps, i.e. as range compression, range-cell migration correction and azimuth compression.

For reference, the measurement was repeated with the conventional quad-polarization mode with separate measurements for each transmitted polarization state.

VI. Measurement Results

The processed SAR images, containing the co- and cross-polarized data sets, can be found in Figs. 5-7. Very eye-catching is the strong backscattering of the fence in the co-polar measurements (HH, VV). This is because the scattering mechanism at the wires of the fence does not rotate the electromagnetic field vector like at dihedral scattering. From a theoretical point of view, the cross-polar measurement results (HV, VH) should be equal and possible variances are an artifact from calibration, the sensitivity of DBF and filtering. Thus, just the mean between the two SAR images is plotted.

The difference plots to the measurement results obtained with the classical quad-polarization mode with separate measurements are depicted in Figs. 8-10. While the mean difference in the co-polarization states is just -29.7 dB in HH (std. dev.: 0.0043) and -28.7 dB in VV (std. dev.: 0.0054), the mean difference in cross-polarization is significantly higher: -21.7 dB in $(|HV| + |VH|)/2$ (std. dev.: 0.0235). Since the mean measured radar cross section differs between the co- and cross-polarized data sets by approximately 6 dB, this deviation is absolutely acceptable. From that it can be concluded that the suggested concept of STFAP is also working for extended targets and polarization.

VII. Conclusion

The concept of STFAP in combination with quad-polarization was firstly verified in [8] for point targets. However, SAR is a sensor for observation of large homogenous areas and a proof with dedicated targets is not enough. Due to that, in this paper the mode of simultaneous quad-polarization was successfully verified with an extended target. Since it is expected that future spaceborne SAR missions will operate with DBF and MIMO modes, this achievement can be seen as a first milestone for the development of such systems.

In the future, further investigations for differences in degree of coherence and cross-correlation interferences between the waveforms are planned. Especially a comparison and performance analysis of the multiple sub-pulse mode with alternative waveform types would be a significant step forward.

References

[1] A. Torre, D. Calabrese, and M. Porfilio, "COSMO-SkyMed: Image quality achievements," in *5th International Conference on Recent Advances in Space Technologies (RAST)*, June 2011, pp. 861–864.

[2] G. Krieger, A. Moreira, H. Fiedler, I. Hajnsek, M. Werner, M. Younis, and M. Zink, "TanDEM-X: A Satellite Formation for High-Resolution SAR Interferometry," *IEEE Transactions on Geoscience and Remote Sensing*, vol. 45, no. 11, pp. 3317–3341, Nov 2007.

[3] A. A. Thompson, A. Luscombe, K. James, and P. Fox, "RADARSAT-2 Mission Status: Capabilities Demonstrated and Image Quality Achieved," in *7th European Conference on Synthetic Aperture Radar (EUSAR)*, June 2008, pp. 1–4.

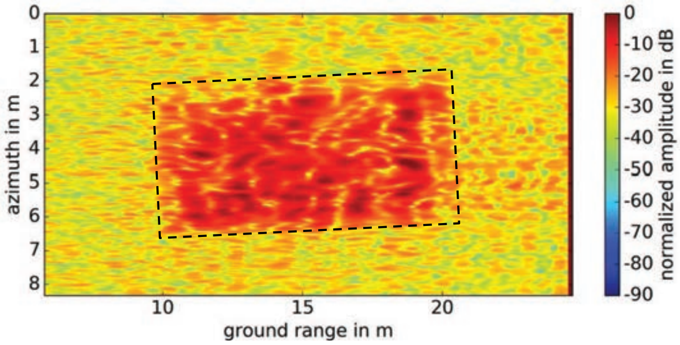

Fig. 5. Focused SAR image in polarization state HH.

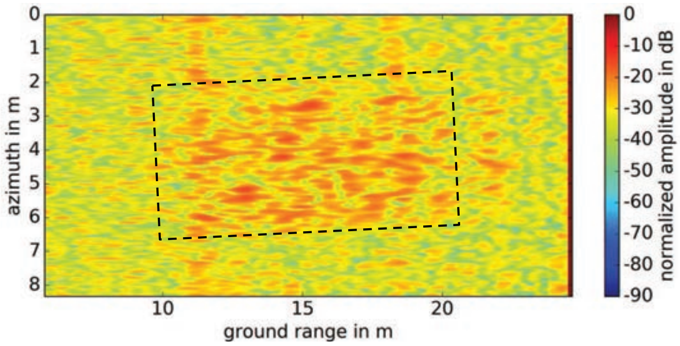

Fig. 6. Focused SAR image in polarization state $(|HV| + |VH|)/2$.

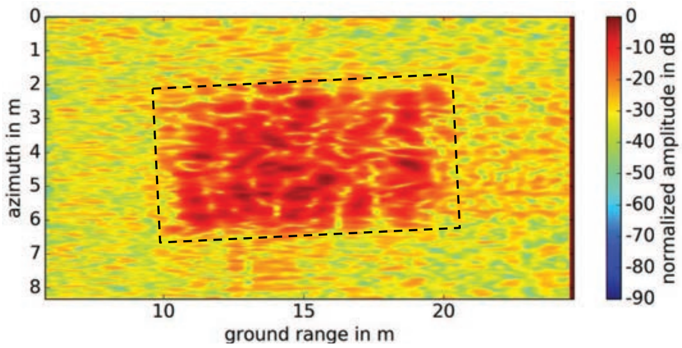

Fig. 7. Focused SAR image in polarization state VV.

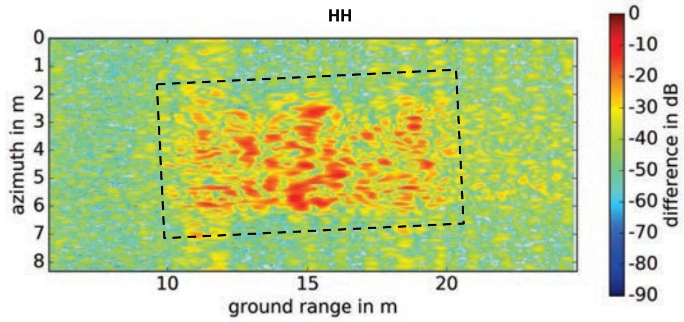

Fig. 8. Difference between individual measurement and MIMO-SAR acquisition in HH polarization (mean: 29.7 dB, std. dev.: 0.0043).

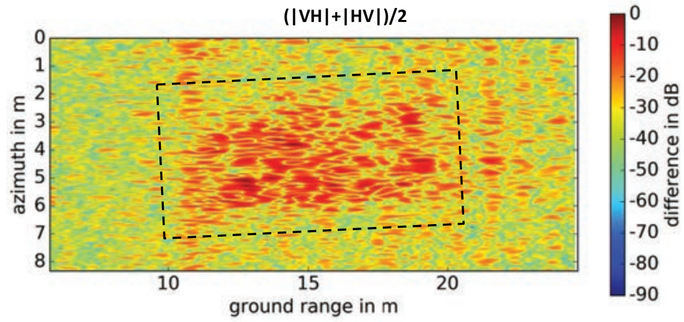

Fig. 9. Difference between individual measurement and MIMO-SAR acquisition in $(|HV| + |VH|)/2$ polarization (mean: -21.7 dB, std. dev.: 0.0235).

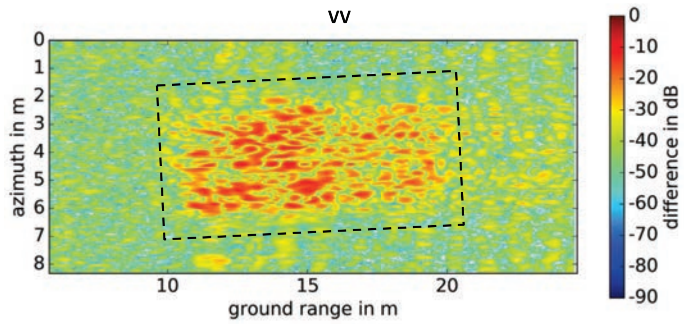

Fig. 10. Difference between individual measurement and MIMO-SAR acquisition in VV polarization (mean: -28.7 dB, std. dev.: 0.0054).

[4] A. Freeman, W. Johnson, B. Huneycutt, R. Jordan, S. Hensley, P. Siqueira, and J. Curlander, "The Myth of the minimum SAR antenna area constraint," *IEEE Transactions on Geoscience and Remote Sensing*, vol. 38, no. 1, pp. 320–324, Jan 2000.

[5] M. Suess and W. Wiesbeck, "Side-Looking Synthetic Aperture Radar System," *European Patent EP 1 241 487*, Sep. 2002.

[6] D. Cristallini, D. Pastina, and P. Lombardo, "Exploiting MIMO SAR Potentialities With Efficient Cross-Track Constellation Configurations for Improved Range Resolution," *IEEE Transactions on - Geoscience and Remote Sensing*, vol. 49, no. 1, pp. 38–52, Jan 2011.

[7] E. Fishler, A. Haimovich, R. Blum, D. Chizhik, L. Cimini, and R. Valenzuela, "MIMO radar: an idea whose time has come," in *Proceedings of the IEEE Radar Conference*, April 2004, pp. 71–78.

[8] T. Rommel, M. Younis, and G. Krieger, "An orthogonal waveform for fully polarimetric MIMO-SAR," in *IEEE Radar Conference*, May 2014, pp. 0887–0891.

[9] I. Hajnsek, M. Shimada, M. Eineder, K. Papathanassiou, T. Motohka, M. Watanabe, M. Ohki, F. De Zan, P. Lopez-Dekker, G. Krieger, and A. Moreira, "Tandem-L: Science Requirements and Mission Concept," in *10th European Conference on Synthetic Aperture Radar, EUSAR*, June 2014, pp. 1255–1258.

[10] G. Krieger, N. Gebert, M. Younis, and A. Moreira, "Advanced synthetic aperture radar based on digital beamforming and waveform diversity," in *IEEE Radar Conference*, May 2008, pp. 1–6.

[11] G. Krieger, N. Gebert, and A. Moreira, "Digital Beamforming Techniques for Spaceborne Radar Remote Sensing," in *6th European Conference on Synthetic Aperture Radar (EUSAR)*, May 2006, pp. 1–4.

[12] M. Younis, T. Rommel, F. Bordoni, G. Krieger, and A. Moreira, "On the Pulse Extension Loss in Digital Beamforming SAR," *Geoscience and Remote Sensing Letters, IEEE*, vol. 12, no. 7, pp. 1436–1440, July 2015.